Reply to "Comment on 'Scanning-probe Raman spectroscopy with single-molecule sensitivity' "

Catalin C. Neacsu,[1] Jens Dreyer,[1] Nicolas Behr,[2] and Markus B. Raschke[3]
[1]*Max-Born-Institut für Nichtlineare Optik und Kurzzeitspektroskopie, D-12489 Berlin, Germany*
[2]*Department of Physics, Humboldt University Berlin, D-12489 Berlin, Germany*
[3]*Department of Chemistry, University of Washington, Seattle, Washington 98195, USA*
(Received 15 March 2007; published 12 June 2007)

In the Comment by Domke and Pettinger [Phys. Rev. B **75**, 236401 (2007)] on our study on "Scanning-probe Raman spectroscopy with single-molecule sensitivity" [C. C. Neacsu *et al.* Phys. Rev. B **73**, 193406 (2006)] the authors raise concerns whether our tip-enhanced Raman response is due to carbon clusters as molecular decomposition products of the malachite green molecules used. Their arguments are based on the different spectral characteristics we observe between the tip-enhanced and far-field Raman response. Here, we show the results of systematic control experiments to support the conclusions drawn by Neacsu *et al.* that all spectral features can be related to malachite green molecules. Comparing Raman spectra for different degrees of near-field enhancement, the absence of spectral changes during bleaching, examining a broad spectral range, and the explicit comparison with Raman signals from carbon impurities validates our original assignment, including the single-molecule response.

DOI: 10.1103/PhysRevB.75.236402 PACS number(s): 78.67.−n, 33.20.Fb, 33.80.−b, 68.37.Uv

In the preceding Comment,[1] Domke and Pettinger question whether in our tip-enhanced Raman experiments[2] the response we observe originates from the malachite green (MG) molecules under investigation, or whether the spectral features have to be assigned to carbon clusters as decomposition products of the MG molecules. Their concerns are largely based on the pronounced spectral differences we observe in case of high field enhancement in the tip-enhanced as compared to the far-field Raman response. In their view the spectral features resemble what has been observed in surface-enhanced Raman scattering (SERS) from carbon clusters. To support our conclusions, we show additional experimental results, discuss our control experiments, and compare with the mode assignment from density-functional theory (DFT). From tip-scattered Raman data for different degrees of enhancement, the analysis of its bleaching behavior from time series experiments, and the explicit comparison with the Raman response from carbon clusters, we conclude that we observe a single-molecule response from MG in Ref. 2.

The authors of the Comment do not question the near-field character of our Raman response, nor the large enhancement obtained in our experiments. In the following, we therefore focus on the demonstration that the Raman response can be assigned unambiguously to MG—even for large enhancement and for the case of the single-molecule response—and is not due to carbonaceous decomposition products. In Fig. 1, for comparison with the far-field spectrum and the strongly enhanced near-field case (a) with an enhancement of 3×10^8 from the original work, we show three additional tip-enhanced spectra [(b)–(d)]. These spectra are taken for the same surface coverage of ~1 ML of MG, but using tips exhibiting different enhancements of (b) 7×10^7, (c) 1×10^7, and (d) 1×10^6, respectively. Even for large enhancements, the signal intensities are weak and the noise is significant in part due to the strong nonlinear dependence of the enhancement with tip-sample distance. We therefore limited the spectral resolution to 25 cm^{-1} for the tip-enhanced experiments.

Evidently, for the weakest enhancements of (d) 1×10^6 and (c) 1×10^7, the spectra closely resemble the far-field response. However, with increasing enhancement of (b) 7×10^7, and most pronounced for (a) 3×10^8, the vibrational modes start to look markedly different. These spectral variations call for the question, as pointed out correctly in the Comment, whether they are due to structural changes and decomposition of the molecules or whether they are indeed intrinsic to MG and a result of, e.g., the large field gradient in the tip-sample gap as we suggested in Ref. 2.

To probe for the appearance of photoreaction products and their signature in the Raman spectra, the evolution of the Raman emission is monitored in time-series experiments. Figure 2 shows consecutive near-field Raman spectra acquired for 1 s each for an enhancement of 1.3×10^7. The molecules bleach on a time scale of ~100 s. During the bleaching, no new spectral features appear. Also, the signal decays with the relative peak amplitudes remaining constant. After complete bleaching, no discernible Raman response can be observed.

The fluctuation observed in the time series is expected given the small number of ~100 molecules probed in the near-field enhanced region under the tip apex. The sum over all spectra (top graph) or the sum of any large enough subset even at later times, i.e., after substantial bleaching, has already occurred, closely resembles the far-field response of MG and thus allows us to attribute the Raman response to malachite green molecules. The same behavior of a gradual and homogeneous disappearance of the Raman response without a relative change in peak intensity is also observed for larger enhancements, i.e., the case where a different mode structure is observed, with in general decreasing decay time constant due to the larger local field. From this, together with the qualitative analysis of the decay in Fig. 2 for an enhancement of 1.3×10^7 or the quantitative comparison of the bleaching decay rates (see below), it can be excluded that in the case of higher enhancement already, the first spectrum in the time series is due to decomposition product—in clear contrast to what is suggested in the Comment. This rules out

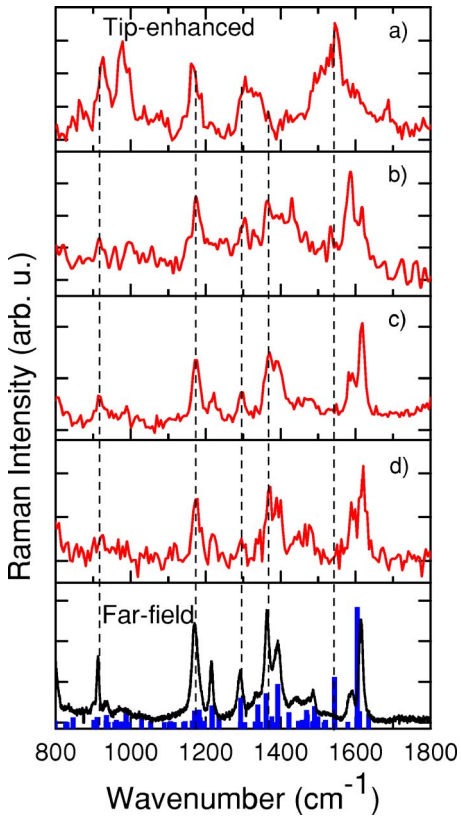

FIG. 1. (Color online) [(a)–(d)] Tip-enhanced Raman spectra for ~1 ML malachite green for different degrees of enhancement in comparison with the corresponding far-field Raman spectrum (bottom graph) and the result of DFT calculation for the mode assignment. The Raman enhancement factors derived are (a) 3×10^8, (b) 7×10^7, (c) 1×10^7, and (d) 1×10^6, respectively, with an experimental uncertainty of a factor of 3–5 for each value. Data are acquired for (a) 1 s, [(b) and (c)] 100 s, and (d) 30 s, respectively. Spectral resolution is 25 cm^{-1} for the near-field and 1 cm^{-1} for the far-field spectra.

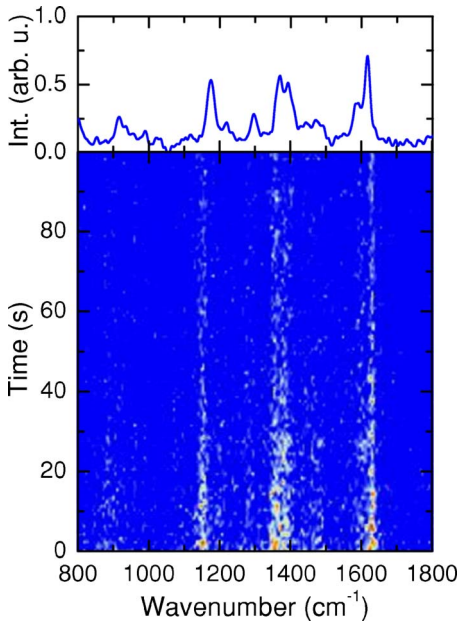

FIG. 2. (Color online) Time series of 100 consecutive near-field Raman spectra (acquired for 1 s each) for ~1 ML MG on Au (Raman enhancement of 1.3×10^7). The Raman spectrum clearly resembles the far-field spectrum. The signal decays to zero due to bleaching. No new spectral features appear from the photoreaction products.

that the spectra for large enhancement shown in Figs. 1(a), 1(b), 2(a), and 2(b) of our original paper are due to carbon clusters or other decomposition products and instead have to be assigned to malachite green.

These results show that at least for monolayer coverages or below, the decomposition products of MG during bleaching do not contribute to the Raman response—irrespective of the level of enhancement considered here. In contrast, if bleaching would lead to photoreaction products with appreciable Raman activity such as carbon clusters, one would expect to see the appearance of new spectral features in the time-series experiments (with the latter being observed for multilayer decomposition of MG as discussed below).

Figure 3 shows the decay kinetics of the spectrally integrated intensity for the Raman time series from Fig. 2. This is shown in comparison to the integral intensity of the region from 1550 to 1650 cm^{-1} encompassing only the two prominent modes (inset). Assuming an exponential decay behavior of $I/I_0=\exp(-t/\tau)$ for the Raman intensity, a decay time $\tau=40\pm5$ s is derived from the fit in both cases.

Our molecular lifetime exceeds the one referred to by the authors of the Comment, deduced from their previous studies[3] by more than 2 orders of magnitude: From our applied laser fluence of 3×10^4 W/cm^2 and the enhancement of the pump intensity of $\sim\sqrt{1.3\times10^7}$, the bleaching would be induced by a local pump fluence of 4.7×10^7 W/cm^2. For comparison, in Ref. 9 a bleaching rate of $\tau=7.3$ s for malachite green Isothiocyanate (MGITC) for a Raman enhancement of 10^6 was observed. Taking into account this difference in enhancement, the 0.5 mW laser power and the numerical aperture of the objective of NA=0.5 used in Ref. 3, our laser fluence under the tip is ~30 times higher than the one in Ref. 3. Taking the different fluences into account shows that our molecular lifetime is ~150 times longer than the one for the MGITC molecules in Ref. 3.

This clearly invalidates the arguments put forward in the Comment, where from extrapolating the bleaching rate from the experiment in Ref. 3, it is stated that our MG molecules should have decomposed before the first spectrum could have been acquired and we should not be able to observe intact MG for the enhancements in our experiments. Moreover, we would like to point out that the calculation in the Comment is wrong because the authors erroneously compare the value for our field enhancement of 5×10^9 which includes the Fresnel coefficient for Au (instead of 3×10^8) with their value which does not include the Fresnel factor.

With regard to the different bleaching rates observed, it should be noted that the bleaching rate is not a characteristic physical quantity universal for a given molecule. Bleaching mechanisms can be quite diverse.[4] They may include irreversible photoinduced or even multiphoton induced reactions such as rearrangements, dissociation and fragmentation, elimination or hydrogen abstraction, or perhaps photo-

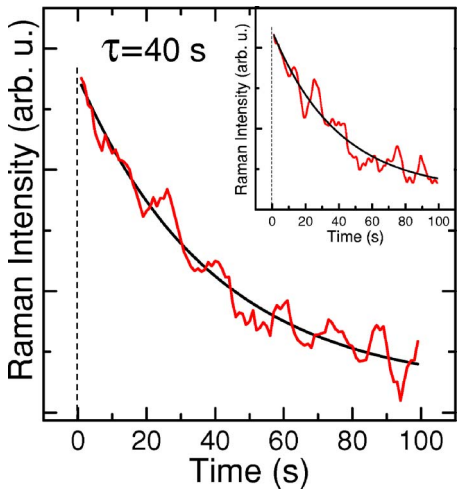

FIG. 3. (Color online) Bleaching kinetics derived from Fig. 2 for the spectrally integrated Raman time series and the region from 1550 to 1650 cm^{-1} (inset). An exponential decay constant of $\tau=40\pm5$ s results for the enhancement of 1.3×10^7 and the incident laser fluence of 3×10^4 W/cm^2 in this experiment.

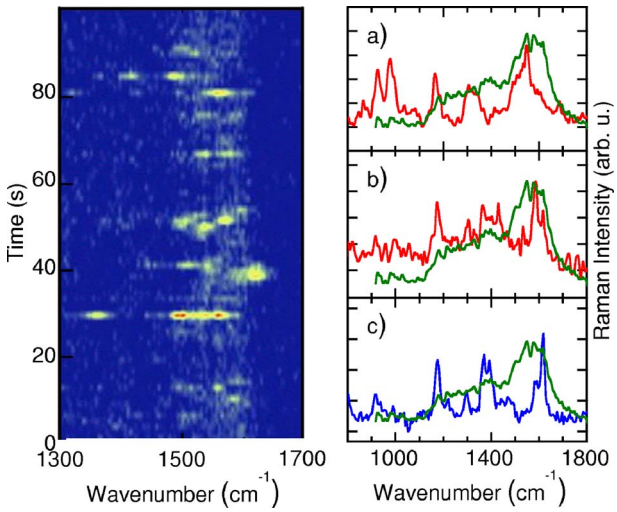

FIG. 4. (Color online) Left: time series of tip-scattered Raman spectra (Fig. 3 in Ref. 2). Right: comparison between sum spectrum of data shown in left panel (olive) and tip-enhanced Raman spectra for different degrees of enhancement [red, (a) and (b)] and sum spectrum of data shown in Fig. 2 blue).

oxidation with ambient oxygen via triplet states. It can depend on, e.g., humidity or cleanliness of tip and sample, and is hence not a useful measure to compare experiments performed under different conditions in different laboratories. What might account for the higher bleaching rate observed in Ref. 3 is that in their study, the authors use a scanning tunneling microscope to manipulate the tip compared to the use of force microscopy in our experiments. With the molecules in addition to the laser field being exposed to an applied tunneling current of 1 nA and local dc bias field of ~150 mV/1 nm$=1.5\times10^8$ V m^{-1}, additional electronic excitation channels are feasible which might enhance the bleaching rate.

Single-molecule response. With regard to our submonolayer and single-molecule response discussed in Ref. 2, the authors of the Comment perform a very misleading analysis. They discuss the time series we observe for the ~0.01 ML sample using a probe tip which exhibits the strongest enhancement of 3×10^8, as if they expect that the modes of the individual spectra shall resemble the far-field emission (Fig. 1 in the Comment). As discussed above for the enhancement of 3×10^8 a different mode structure of MG is expected compared to the far-field response. The sum over the times series shall therefore resemble an ensemble spectrum for large near-field enhancement, rather than the far-field Raman spectrum as claimed by the authors of the Comment. In Fig. 4, we show the sum spectrum (right) for the single-molecule response for the 100 s time series (left) in comparison with ensemble spectra of ~100 molecules probed for 1 s. In assessing the resemblance of the spectral characteristics, it has to be considered that at low coverage, the molecules have more degrees of freedom to dynamically change orientation and they can diffuse in and out of the apex-confined probe region. However, given the weak response, the signal detected can only be expected to emerge from the region of largest enhancement. Sampling over this regions with its lateral variation in enhancement would give rise to further broadening of the strongly enhanced near-field response compared to the far-field case. Therefore, while individual spectral features at positions in accordance with the strongly tip-enhanced near-field response are clearly observed in the time series, it is not surprising that the sum spectrum no longer exhibits clearly resolved lines. With the diffusing molecules probing the spatial variation of the enhancement under the tip, this corresponds to an extreme case of inhomogeneous broadening. This interpretation is corroborated considering, e.g., the improved resemblance of the peak in the 1550–1600 cm^{-1} region of the single-molecule sum spectrum with the sum of the two near-field spectra [in (a) and (b)] of different enhancement.

Note that in the time series in Fig. 4, the apparent bleaching rate seems reduced compared to what is expected from the analysis of the ensemble bleaching discussed above. This is a result of the low surface coverage where new molecules directly neighboring the tip-sample gap can diffuse into the near-field enhanced region.

The temporal variation and its probability distribution of the corresponding integrated intensity of the 1480–1630 cm^{-1} region are shown in our original work[2] in Fig. 3(b). As the authors of the Comment emphasize and which has been shown more quantitatively recently,[5] a Poisson-like probability distribution for a small sample set has, in general, to be greeted with scepticism when used as the sole argument for single-molecule signature. However, as discussed in Ref. 2 and in contrast to the claim of the authors, our single-molecule assignment of the Raman response in Fig. 4 originates from the combination of three experimental conditions and observations: First, from the use of a dilute submonolayer coverage where we expect on average only one molecule under the tip apex region of ~100 nm^2. Second and most importantly, the signal intensity observed corresponds to that of an ~1, 2, or 3 molecules as derived from comparison with the far-field and tip-enhanced

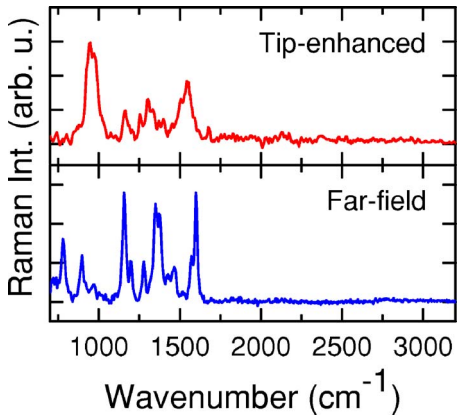

FIG. 5. (Color online) Tip-enhanced (enhancement $\sim 10^8$) and far-field MG Raman spectrum for ~ 1 ML of MG including the higher-energy spectral range. Although spectrally different from the far-field response, the absence of any spectral signature above 1800 cm^{-1} for the tip-enhanced response contrasts the observation for carbonaceous species.

ensemble response of a full monolayer. In that case and considering that the "hot-spot" SERS model analyzed in Ref. 5 is in fact different from the TERS case,[9] the analysis of the intensity distribution is meaningful. Therefore and third, the occurrence of discrete peaks in the probability distribution which is already evident from visually inspecting the time series of integrated intensities [dashed lines in Fig. 3(B) in Ref. 2] *supports* the interpretation of the single-molecule response. The details of the histogram, however, clearly depend on the binning procedure especially for such a small data set. The conclusion whether the distribution is Poissonian—which we do not draw—would, as pointed out by Le Ru *et al.*,[5] require larger data sets.

Hence, it is the combination of these three observations together with the series of experiments discussed above and the control experiments below that lead us to the conclusion that we observe the Raman response of a single MG molecule.

Carbon Raman response. In the following, results of control experiments are discussed which further support the conclusion of the absence of carbon contamination or decomposition products to have affected the Raman response in our experiments that are shown here and in Ref. 2. Figure 5 shows Raman spectra for the energy range beyond 2000 cm^{-1} for an enhancement of $\sim 10^8$. Evidently, even for high enhancement our near-field spectra from ~ 1 ML MG do not show Raman bands at frequencies above 1750 cm^{-1}. In that region, carbon clusters and carboniferous decomposition products are known to exhibit Raman bands of appreciable intensity.[6,10]

For comparison, in the following we analyze a carboniferous Raman response. Figure 6 shows a time series of consecutive tip-enhanced Raman spectra acquired for 1 s each from a multilayer of photodecomposed MG. The observed behavior is characteristic for Raman scattering from carbon clusters and very distinct from the spectral response discussed above for monolayer or submonolayer MG in several ways: First, in accordance with previous observations,[6–8] including those from the authors of the Comment, the Raman response is comparatively large and fluctuates rapidly and in an uncorrelated way. This behavior is very different compared to all our observations for MG, including the single-molecule response. Second, a distinct spectral feature emerges around 2000 cm^{-1} which has been assigned to, e.g., modes within the segments of carbon chains. In contrast, even for very high enhancement our near-field spectra from 1 ML MG no Raman bands can be observed at frequencies above 1750 cm^{-1}.

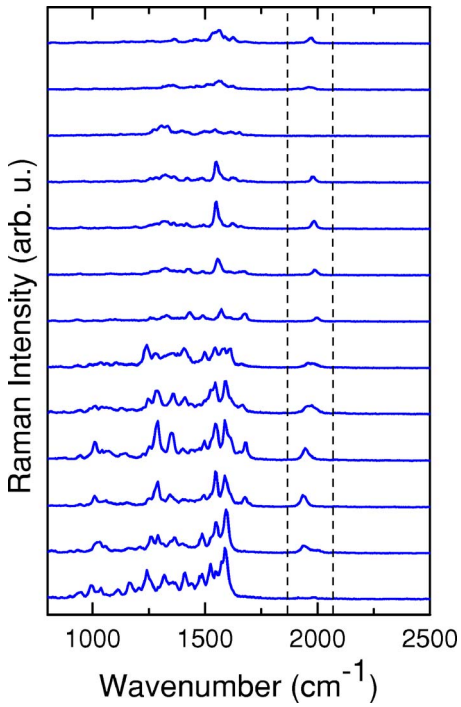

FIG. 6. (Color online) Time series of consecutive near-field Raman spectra acquired for a photodecomposed MG multilayer. The large and uncorrelated spectral fluctuations and the band at 1870–2100 cm^{-1} are characteristic for carbon clusters.

Third, this carbon Raman response is due to extended carbon chains and aggregates which can readily form by multilayer MG decomposition. In contrast, at ambient temperatures, one would expect that the bleaching of monolayer and submonolayer coverages (<0.01 ML for our single-molecule experiment) leads to smaller molecular fragments and subsequently to a dilute surface carbon distribution. Fourth, large Raman cross sections are reported for carbon clusters and carbonaceous species in SERS consistent with the strong signals observed in Fig. 6. Should they have formed in our experiments shown here or in Ref. 2, they would have manifested themselves in an appreciable Raman response in the time series experiments.

Mode analysis. The DFT calculations we performed and discussed in Ref. 2 allow for identification of the spectral features in the far-field spectrum of Fig. 1(d)). Furthermore, the calculations show that the new spectral features seen in the near field spectrum [Fig. 1(a)] may correspond to vibrational modes of MG, which we briefly discuss here.

Several Raman features are present in both the far-field and the strongly enhanced near-field spectra. Prominent Ra-

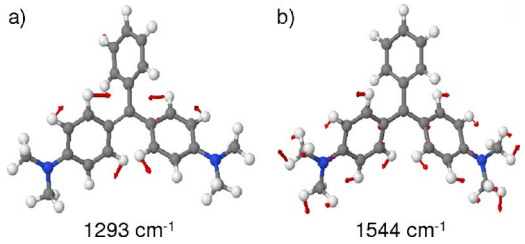

FIG. 7. (Color online) Illustration of calculated Raman active normal modes of the MG molecule at (a) 1293 cm^{-1} and (b) 1544 cm^{-1}. (a) In-plane C—H deformation mode together with C—C stretching of the methane group. This mode is observed in all near-field spectra irrespective of the enhancement level. (b) skeletal stretching motions combined with in-plane C—H bending motions of the conjugated di-methyl-amino-phenyl rings. This mode is not present in the FF spectrum, but its intensity grows with the near-field enhancement (see Fig. 1).

man modes at 920, 1170, and 1305 cm^{-1} appear for all enhancements. In the spectral region of 910–980 cm^{-1}, several vibrational modes, typically characterized by in-plane skeletal bending and/or out-of-plane C—H motions, are found. The 1170 cm^{-1} mode may be assigned to a methyl group rocking mode or an in-plane C—H bending mode of the phenyl ring. Around 1300 cm^{-1}, in-plane C—H deformation modes and C—C stretching modes of the methane group are located [Fig. 7(a)].

Among the characteristic near-field enhanced modes, e.g., the peak at 1365 cm^{-1}, which is very strong in the far field spectrum, but decreases with increasing enhancement, can be assigned to combination of C=C stretching motions of the aromatic ring. In contrast, the prominent peak at 1544 cm^{-1} which dominates for the highest enhancement is very weak for small enhancements or in the far-field spectra. Here, the calculation shows a mode characterized by stretching motions combined with in-plane C—H bending motions of the conjugated di-methyl-amino-phenyl rings [Fig. 7(b)]. The two modes at 1585 and 1615 cm^{-1}, which can be assigned to C=C stretching vibrations of the phenyl ring, decrease with enhancement.

This change in both intensity and spectral signature with increasing near-field enhancement together with the vibrational analysis shows that the peaks observed may well correspond to vibrational modes of MG, in contrast to the claims made in the Comment, whereby different selection rules must apply for the Raman spectra obtained under condition of high enhancements.

In summary, with the results presented we believe to have refuted the proposed alternative interpretation based on "carbonaceous species" of our tip-enhanced and single-molecule Raman response as brought forward by Domke and Pettinger.[1] We regret that in our original paper, we did not provide more experimental details and thank the authors of the Comment for the opportunity to clarify the important issue of the assignment of the Raman spectra in this Reply. We would like to emphasize, however, that the differences of the spectral characteristics of the tip-enhanced versus the far-field response are surprising and the mechanism responsible for it still remains to be understood. Given the inherent experimental challenges involved, the data do lack the precision to arrive at a definite conclusion about the mechanism at this stage.

Note added in proof. Recently, similar observations have been made in related experiments by Zhang *et al.*[12] and Ward *et al.*[13]

[1] K. Domke and B. Pettinger, Phys. Rev. B **75**, 236401 (2007).
[2] C. C. Neacsu, J. Dreyer, N. Behr, and M. B. Raschke, Phys. Rev. B **73**, 193406 (2006).
[3] B. Pettinger, B. Ren, G. Picardi, R. Schuster, and G. Ertl, Phys. Rev. Lett. **92**, 096101 (2004).
[4] X. S. Xie and J. Trautman, Annu. Rev. Phys. Chem. **49**, 441 (1998).
[5] E. C. Le Ru, P. G. Etchegoin, and M. Meyer, J. Chem. Phys. **125**, 204701 (2006).
[6] A. Kudelski and B. Pettinger, Chem. Phys. Lett. **321**, 356 (2000).
[7] G. Picardi, Ph.D. thesis, Freie Universität Berlin 2003.
[8] P. Moyer, J. Smith, L. Eng, and A. Meixner, J. Am. Chem. Soc. **122**, 5409 (2000).
[9] The bispherical SERS model (Ref. 5) differs from the TERS geometry in two significant ways: the molecules are randomly distributed in three dimension across the spheres, whereas in TERS the molecules are spatially more confined—now using the bispherical picture—in two-dimensional in the sagital plane intersecting the bispheres. In addition, compared to the bispherical geometry, the antennalike geometry of the elongated tip results in a strong radial field confinement in the surface plane as we showed previously (Ref. 11). Hence, in TERS with 30 events in 100 s in our case single-molecule detection is significantly more probable and scaling with concentration can be observed even for on average one molecule per "hot spot" which would be challenging for a similar SERS geometry, as shown in Ref. 5.
[10] C—H stretch modes near 3000 cm^{-1} of MG are not resonantly enhanced and their absence in the spectra is therefore not surprising.
[11] R. M. Roth, N. C. Panoiu, M. M. Adams, R. M. Osgood, C. C. Neacsu, and M. B. Raschke, Opt. Express **14**, 2921 (2006).
[12] W. Zhang, B. S. Yeo, T. Schmid, and R. Zenobi, J. Phys. Chem. C. **111**, 1733 (2007).
[13] D. R. Ward, N. K. Grady, C. S. Levin, N. J. Halas, Y. Hu, P. Nordlander, and D. Natelson, Nano. Lett. (to be published).